

Use of data-driven design for the development of knob-shaped handles in the context of impedance measurements

Tassilo Schröder, Andreas Lindenmann, Sophia Hehmann, Andreas Wettstein, René Germann, Thomas Gwosch, Sven Matthiesen *

Karlsruhe Institute of Technology (KIT), IPEK - Institute of Product Engineering, Kaiserstraße 10, 76131, Karlsruhe, Germany

A B S T R A C T

Keywords:

Hand-arm vibration
Grip force
Measuring handle

It can be inferred from hand-arm impedance analyses that the grip forces of users have a great influence on the transmitted vibrations. To determine this influence on test benches, the state of research suggests a cylindrical measuring handle. Since this shape is not suitable for all power tool handles, we develop a design for a knob-shaped measuring handle. The grip force applied to an orbital sander was measured in a test person study. The recorded data was combined with a 3D scan and evaluated by an algorithm which determined the separation plane of the measuring handle to integrate the force sensors. This plane is perpendicular to the vector of the subjects' grip forces. Furthermore, it divides the knob-shaped handle of the sander primarily vertically. The determination of the separation plane enables the design of a knob-shaped measuring handle for grip force measurement to analyze the hand-arm impedance of an overlying hand position.

1. Introduction

The long-term vibration exposure of the hand-arm system can lead to vascular and neuronal health issues (I 2057 Blatt 2: Einwirk, 2016; Dong et al., 2006a; Burstrom, 1997; 5349-1:2001: M, 2001; Wahl et al., 2019; Rademacher et al., 1993; Kihlberg and Hagberg, 1997; Vergara et al., 2008; Bovenzi, 1994; Griffin, 1996; Verberk et al., 1985; Edwards et al., 2020; Hussein et al., 2019; Vihlborg et al., 2017; Krajnak, 2018; Nataletti et al., 2008). Several studies have linked these vibration-related health issues of the hand-arm system to the use of power tools (Wahl et al., 2019; Kihlberg and Hagberg, 1997; Vergara et al., 2008; Verberk et al., 1985; Edwards et al., 2020; Vihlborg et al., 2017; Krajnak, 2018). In 2018, Krajnak published a review concerning the association between occupational vibration exposure and health effects (Krajnak, 2018). In terms of hand-transmitted vibrations, Krajnak gave an overview of the state of research regarding vibration exposure in various industries. In the industrial sector of manufacturing, the majority of employees is exposed to hand-transmitted vibrations, since different types of power tools, such as grinders, drills, and sanders are used (Krajnak, 2018). These hand-transmitted vibrations caused by the use of power tools lead to vascular and neuronal effects like the reduction of the blood flow and tactile sensitivity (Krajnak, 2018). The Raynaud syndrome or so-called vibration white finger syndrome is one of the vascular diseases caused

by vibration exposure (Wahl et al., 2019; Rademacher et al., 1993; Bovenzi, 1994; Vihlborg et al., 2017; Krajnak, 2018). Besides this syndrome, there are other hand-related neuronal and muscular long-term consequences of vibration exposure, e.g. the carpal tunnel syndrome (Wahl et al., 2019; Vihlborg et al., 2017).

Concerning the carpal tunnel syndrome, Vihlborg et al. published the results of a field study on the association between vascular, neuronal, or muscular diseases and the use of vibrating tools in the Swedish industry (Vihlborg et al., 2017). In this study, 68 full-time employees from the mechanical industry were interviewed about vibration-related symptoms using a questionnaire. In addition, the health status of the employees was examined with regard to vibration-related diseases (Vihlborg et al., 2017). Subjects who showed symptoms of vibration-related diseases were examined again after three years. Vihlborg et al. identified the use of straight grinders as the main source of vibration exposure and measured the vibration level of this power tool with a tri-axial accelerometer (Vihlborg et al., 2017). In summary, 21% of the subjects in the field study showed symptoms of vibration-related disorders, with carpal tunnel syndrome appearing to be overrepresented (Vihlborg et al., 2017). DIN EN ISO 5349-1 is an established standard for the measurement of vibration exposure (5349-1:2001: M, 2001). A central aspect of this ISO standard is the so-called a_{hv} -value, which is represented by the square root of the sum of the squared RMS value of

* Corresponding author.

E-mail address: sven.matthiesen@kit.edu (S. Matthiesen).

the frequency weight acceleration values from each direction.

Based on the a_{hv} -value, the vibration dose value can be calculated (5349-1:2001: M, 2001). In this context, Wahl et al. published a manuscript in 2019 in which they plead for a revision of the German occupational safety guidelines under consideration of ISO-5349-1 among other standards (Wahl et al., 2019). In summary, the current state of research shows that the vibration exposure of the hand-arm system in the work of power tools is a recent problem and leads to serious health issues. To understand and prevent these vibration-related diseases, the biodynamic response of the hand-arm system to vibration exposure must be investigated (5349-1:2001: M, 2001; Adewusi et al., 2010). In addition, the investigation of the biodynamic responses of the hand-arm system is essential for the development of vibration damping devices and hand-arm vibration simulators for the assessment of power tools (Rakheja et al., 2002; Scarpa et al., 2005). The mechanical impedance of the hand-arm system is an established quantity for measuring the biodynamic responses of the hand-arm system to vibration exposure (Dong et al., 2006a; Matthiesen et al., 2014; N 45679:2013-02: Mechan, 2013; Lindenmann and Matthiesen, 2019; Dong et al., 2001; Dong et al., 2006b; Dong et al., 2013; Donget al., 2012; Aldien et al., 2005a). The mechanical impedance describes the resistance of the hand-arm system against vibration (Dong et al., 2005; Matysek and Kern, 2009). The impedance can be calculated for translational and angular vibrations (Dong et al., 2005; Matysek and Kern, 2009). In the case of translational vibrations, the impedance is the complex frequency-dependent quotient of the force amplitude and the velocity (Dong et al., 2005). Concerning the rotatory impedance, the complex frequency-dependent quotient of the torque amplitude and the angle acceleration have to be calculated (Matysek and Kern, 2009). To measure and evaluate the impedance of the human hand-arm system under laboratory conditions, a test bench with a measuring handle attached to a shaker system can be used (Dong et al., 2006a; Lindenmann and Matthiesen, 2019; Dong et al., 2001; Dong et al., 2006b; Dong et al., 2013; Donget al., 2012; Welcome et al., 2004a; Matthiesen et al., 2018; 10819:2019-5, 2019). The impedance of the hand-arm system depends, among other things, on the coupling force, which the user applies to the handle as the source of vibration exposure. The coupling force can be defined as the sum of the gripping and the pressing force (N 45679:2013-02: Mechan, 2013; Kaulbars and Lemerle, 2002; Steffen and Kaulbars, 2017; Kaulbars, 2006).

Since the pressing force is measured by sensors attached to the shaker system, the used measuring handle has to be able to measure the grip forces applied by the subject. For this purpose, DIN EN ISO 10819 proposes the use of a cylindrical handle divided into two half cylinders with force sensors in between (Dong et al., 2006a; 10819:2019-5, 2019). This design of the measuring handle is current state of research (Dong et al., 2001, 2006a, 2006b, 2013; Lindenmann and Matthiesen, 2019). Fig. 1 shows the suggested measuring handle taken from (10819:2019-5, 2019).

As can be seen in Fig. 1, the geometry of the established measuring handle is suitable for representing power tools with a power grip but is unsuitable for power tools that have a knob-shaped handle. An example of a power tool with a knob-shaped handle is the random orbital sander. In regard to the state of research, sanders are relevant sources of hand-transmitted vibrations (Rademacher et al., 1993; Vergara et al., 2008; Verberk et al., 1985; Vihlborg et al., 2017; Krajnak, 2018; Xu et al., 2011). In addition, DIN EN-ISO 5349-1 refers, among other things, to a gripping position where the hand lies on the top of the handle (5349-1:2001: M, 2001). It can be assumed that for a knob-shaped handle, the gripping position results in a different coupling between the hand and the handle. Due to the shape of the handle, the hand rests on the top of the handle instead of closing around the handle as would be the case with a cylindrical handle, possibly resulting in a lower gripping force.

Since the impedance of the hand-arm system depends on the gripping force, it is expected to change due to the shape of the handle

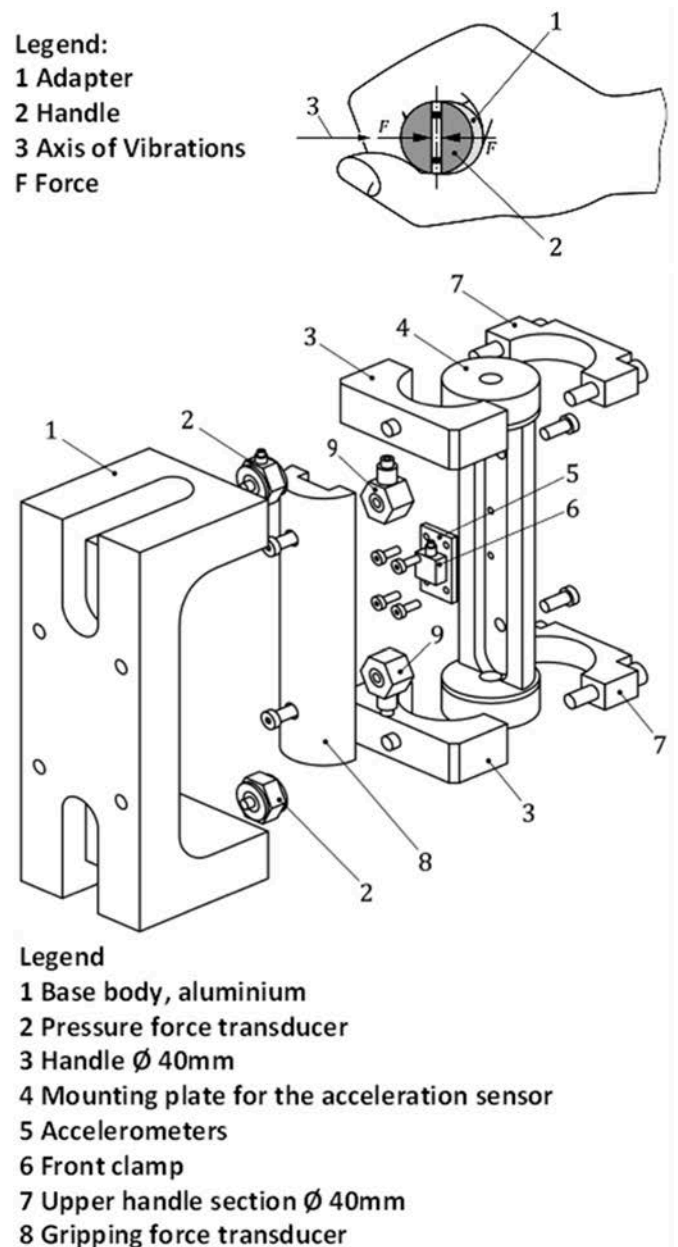


Fig. 1. Measuring handle for grip forces, top view and exploded view (10819:2019-5, 2019).

(5349-1:2001: M, 2001).

In case of a cylindrical handle the influence of different handle diameters on the grip force could be shown by Aldien et al. (2005b). For this purpose three cylindrical handles with different diameters were equipped with a force measuring foil in order to measure the distribution of the gripping and contact force on the palm and the fingers (Aldien et al., 2005b). From the obtained results Aldien et al. conclude that for a larger handle size the subject is encouraged to apply the grip force over the entire hand surface (Aldien et al., 2005b). In a similar study Welcome et al. also equipped cylindrical handles with a force measuring foil in order to measure the grip, push and contact forces of 10 male subjects at different handle diameters (Welcome et al., 2004b). Hereby the results of Welcome et al. suggest a linear dependence between the grip forces and handle diameter. In this context Welcome et al. suggest that smaller handle diameters lead to a higher hand-handle interface pressure, which is consistent with the conclusions of Aldien et al. (Welcome et al., 2004b).

The findings of Aldien et al. and Welcome et al. support the assumption of a different coupling for knob-shaped handles, since for a knob-shaped handle, the handle's dimensions are even larger (Aldien et al., 2005b).

In further studies by Marcotte et al. and Aldien et al. the influence of the diameter of a cylindrical measuring handle on the mechanical impedance of the hand-arm system was studied (Aldien et al., 2005a; Marcotte et al., 2005). Hereby, Marcotte et al. varied the diameter of the measuring handle in three different steps of 30, 40 and 50 mm in a study with seven adult male subjects. In this study, a significant influence of the handle diameter on the mechanical impedance was found (Marcotte et al., 2005). Therefore, Marcotte et al. suggest that the handle diameter should be considered along with other extrinsic factors, when measuring mechanical impedance (Marcotte et al., 2005). These findings are supported by the results of Aldien et al. which also show a remarkably higher magnitude of mechanical impedance for larger diameters of the measuring handle (Aldien et al., 2005a).

The variation of the handle's the diameter of the established cylindrical handle shows a considerable influence on the mechanical impedance, it can be assumed that the shape of the measuring handle affects the mechanical impedance as well.

In order to this assumption 2011, Xu et al. measured the mechanical impedance of the hand for vibrations exposed normal to the palm referring to the vibration exposure of a random orbital sander plate (Xu et al., 2011). For this purpose, the third octave bands with center frequencies from 16 to 1000 Hz were introduced to the hand-arm system of ten subjects by pressing their palms against a vibrating aluminum platform. In their manuscript, Xu et al. showed that the distributed biodynamic response of the hand varied across the hand and with the applied hand forces (Xu et al., 2011). In this context, Xu et al. point out that the geometric feature of the hand-tool interface could affect the vibration transmissibility, since the fingers are better coupled to a cylindrical handle than to a flat plate (Xu et al., 2011). Here Xu et al. consider the flat surface as an approximated simulation of the orbital sander (Xu et al., 2011). However, in the study by Xu et al. no gripping force could be applied due to the flat surface on which the hand was placed.

According to the current state of research, an influence of the handle geometry on the mechanical impedance can be assumed. The knob-shaped handle represents a common handle shape in power tools such as the random orbital sander. The approximate simulation of such handles on test benches by a flat surface does not allow to apply gripping forces that affect the mechanical impedance of the hand-arm system and that are influenced by the geometry of the handle. Therefore, a knob-shaped measuring grip is required for the grip force measurement.

In the current state of research, there is no proper design for a knob-shaped measuring handle. A main concern is the angular position of the separation plane that divides the measuring handle to place the force sensors for gripping measurement in between (Schroder et al., 2020). In (Schroder et al., 2020), a method for determining the angular position of this separation plane of a knob-shaped measuring handle is discussed. To measure the biodynamic response, a handle using the example of an orbital sander is suggested. The method proposed in (Schroder et al., 2020) determines the angular position of the separation plane for the measuring handle. For this purpose, Schroder et al. (2020) use an optimization algorithm that extracts the angular position of the separation plane from experimental data. The algorithm transforms the 3D model of the orbital sander handle into a 2D projection. The optimized angular position of the separation plane is then transformed back into the 3D model of the orbital sander handle. However, this transformation in (Schroder et al., 2020) only considers the back view of the handle, which is defined as the x-y plane. Consequently only the projection of the separation plane's edge in the x-y plane is calculated. In this context, the z-direction is considered linear and runs straight from the back to the front through the handle. However since the separation plane can have an angular offset in two spatial directions, its angular orientation must

also be determined in the top view of the handle. Hence the projection of the edge of the parting plane in the plan view, defined as the x-z plane, must be calculated. . With the angular position of both edges, a resulting separation plane can be calculated. Therefore, the specific main question of the manuscript is: How is the angular position of the separation plane in knob-shaped measuring grips oriented in three dimensions and how can this position be determined? Furthermore, it must be clarified how the pressing force that the power tool exerts against the surface of a workpiece affects the angular orientation of the separation plane. The analysis for answering these questions was done using the example of an orbital sander.

2. Methods

A study for three-dimensional determination of the separation plane was already published in (Schroder et al., 2020) through a two-dimensional perspective. This manuscript aims to analyze the results from a three-dimensional perspective. This section describes the test setup, the test subjects, and the test procedure. The data of the study is analyzed more in depth, as the method of evaluation is extended from a 2D to a 3D approach. The study considers 30 subjects, whose grip forces were measured in the gripping of an orbital sander through use of a force measuring foil. The measured forces were evaluated in the main direction of the resulting grip force. Since the components of the grip force cancel each other out in the center of the palm (N 45679:2013-02: Mechan, 2013), the main direction of the grip force includes two force vectors directed against each other. In the data analysis, the angular orientation of these vectors was determined in regard to the x-y and x-z planes. This analysis leads to a median angle of the separation plane for splitting of the measuring handle over all 30 subjects.

2.1. Test subjects

The study was conducted with 30 healthy subjects (27 male and 3 female) aged 18–40 years. To record the subjects' age, bodyweight, and body size, we used a clustering which split the age, bodyweight, and body size into five different range clusters. This clustering was done in respect of a higher anonymization of the subjects' data, since the subjects only had to sort themselves into a range cluster instead of revealing their specific age, bodyweight, and body size. The number of subjects in each cluster is given in Table 1.

All subjects were right-handed and said that they were using power tools regularly (1 daily, 7 weekly, 18 monthly, 4 yearly). The data on the subjects' regular use of power tools is limited in its explanatory power since we only asked the subjects' experience in using power tools in general. The test setup used contained two static tasks with a switched-off sander and a grinding task in which only one pattern had to be followed. The use of power tools was only generally queried among the subjects. We considered that under these testing conditions, the subjects' experience in using power tools had little influence on the forces applied. No further questions were therefore asked regarding the use of specific power tools. For each subject, a set of anthropometric properties as given in DIN EN ISO 7250-1 and depicted in Fig. 2 were recorded (7250-1:2017: W, 2017). Table 2 lists the values for the anthropometric

Table 1
Clustering of age, bodyweight, and body height.

Age [years]	Number of subjects	Body height [cm]	Number of subjects	Bodyweight [kg]	Number of subjects
14–18	0	<160	1	<55	0
18–25	14	160–170	1	55–70	9
25–40	16	170–180	15	70–85	14
40–60	0	180–190	8	85–100	6
60–80	0	>190	5	>100	1
Sum	30	Sum	30	Sum	30

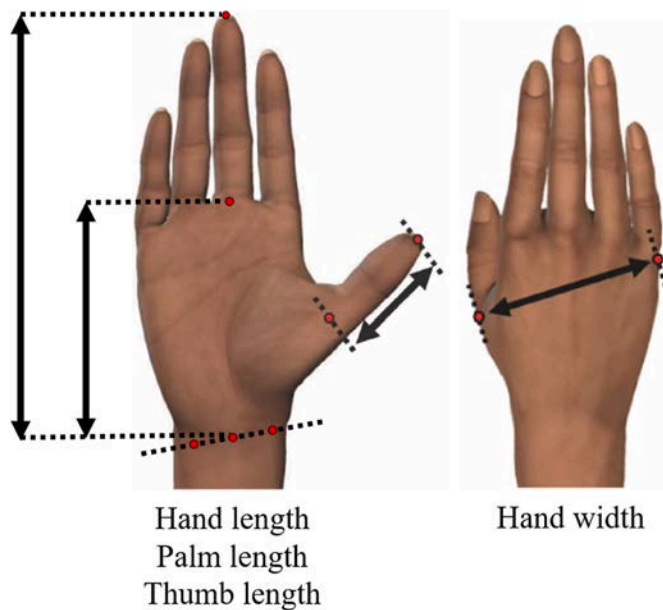


Fig. 2. Anthropometric characteristic of the human hand according to DIN EN ISO 7250-1. The illustration of the hand is based on DIN EN ISO 7250-1 (7250-1:2017: W, 2017).

Table 2
Physical characteristics of the 30 subjects, taken from (Schröder et al., 2020).

Characteristic	Lower quantile [mm]	Median [mm]	Upper quantile [mm]	Standard deviation [mm]
Hand Width	100	102.5	109.25	6.2
Hand Length	181	190	191.2	9.9
Palm Length	103	106.5	110	6.7
Thumb Length	60	65	67	6.9

properties for all subjects. The anthropometric characteristics of the test subjects are within the range of standard values for German subjects given in DIN CEN ISO/TR 7250-2 (O/7250-2N, 2013). All recorded data

were anonymized. The subjects were informed about their rights as well as the form of data acquisition.

2.2. Test setup

For determination of the grip forces on power tools, previous studies by Kalra et al. (2015) and Welcome et al. (2004a) investigated the suitability of force measuring foils which can be applied to the power tool handles. The study conducted by Kalra et al. showed that resistive force measuring foils lack reproducibility. On the other hand, the study conducted by Welcome et al. who used capacitive sensor foils showed low scattering. Further studies conducted by Kaulbars (2006) and Kaulbars and Lemerle P (Kaulbars and Lemerle, 2002). showed the use of capacitive force sensing foils for determination of grip forces on grinders, tampers, and demolition hammers. Furthermore Matthiesen et al. used a force measuring foil for measurement of grip force at an orbital sander in 2017 (Matthiesen and Uhl, 2017).

For the present study on the determination of grip forces on knob-shaped, battery-powered orbital sanders, DBO180U (Makita Corporation, Anjo, Aichi, Japan) was used. The technical data of the sander can be found in (Makita Werkzeug GmbH, 2021). The device and a 3D model of its handle geometry together with the defined coordinate directions is given in Fig. 3. The left side of Fig. 3 shows the device used in the study. The device's handle is surrounded by the projection planes of the initial coordinate system, the planes highlighted in red are the x-y and x-z planes that were considered for the determination of the grip forces. The right side of Fig. 3 shows a 3D model with the corresponding dimensions of the sander handle. The 3D model shown was obtained by scanning the handle geometry with a 3D scanner (HandySCAN-3D, Creaform GmbH, Egenhausen, Germany).

For the manual experiment, the device was equipped with a capacitive force measuring foil on the main gripping surface (pliance-xf-32 with 16x10 element foil, novel GmbH, Munich, Germany). The foil consists of individual pressure elements in a grid arrangement. The elements can measure the mechanical pressure acting on it. The sensor foil was carefully oriented in order to achieve full surface coverage for all subjects. No adjustments were made during the study so that the foil element location and orientation remained consistent for all subjects. The test setup is depicted in Fig. 4. The subjects were standing upright and were working on a level plywood board. The workpiece was raised at a height of 800 mm for all subjects. The subjects were provided with

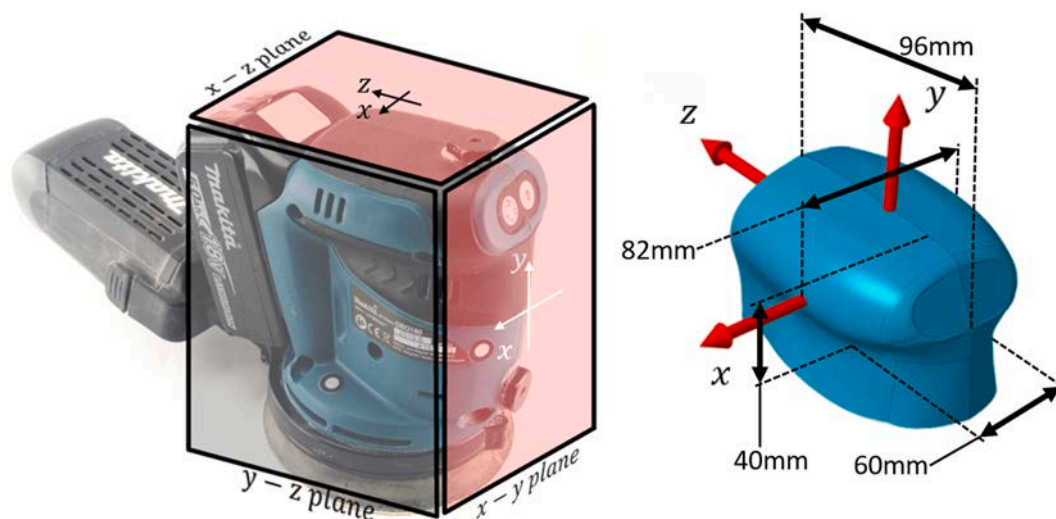


Fig. 3. The left side shows the random orbital sander, which was used in the study, surrounded by the projection planes according to the initial coordinate system of the sander. The planes used for the determination of the grip force are highlighted in red. The right side shows the corresponding coordinate directions defined for the used orbital sander and the dimensions of the sander handle. The 3D model of the sander handle was created using the HandySCAN-3D provided by Creaform GmbH, Egenhausen, Germany. (For interpretation of the references to color in this figure legend, the reader is referred to the Web version of this article.)

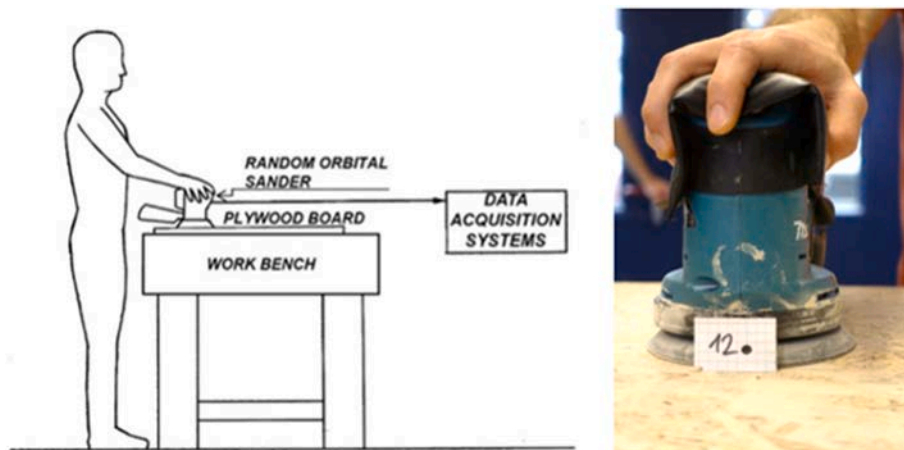


Fig. 4. Schematic drawing of the test setup and photo of the orbital sander.

an instructional display guiding them through the individual steps of the study. The data for the force measuring foils was acquired by the control unit of the force measuring foil itself at a rate of 60 Hz.

with the applied force measuring foil gripped by subject 12 (Schroder et al., 2020).

2.3. Test procedure

At the beginning of the experiment, the subjects were introduced to the general test procedure and aim of the study. Then, the anthropometric properties were recorded. Next, the subjects were allowed to familiarize themselves with the test setup. The subjects were allowed to freely work on the plywood board for 2 min with an unmodified sander in order to get a sensation of the gripping and pushing forces required for operation. In the subsequent step, the participants were handed the orbital sander with the force sensing foil. As part of the study, the subjects had to perform three different tasks with the random orbital sander. The first task involved holding the sander statically with outstretched arm for 10 s. In the second task, the subjects gripped the switched-off device while pressing on the plywood plate for 20 s. In this pressing task, only the first trial was recorded to assess the intuitive, unaffected gripping manner of the subject. In the third task, the sander equipped with the sensor foil was switched on and the subject ground the plywood plate according to a specified pattern based on DIN EN ISO 28927-3 and corresponding to a horizontal figure of eight with a circular diameter of 100 mm (28927-3:2010-0, 2010). According to DIN EN ISO 28927-3, this pattern had to be ground within 4 s. For this purpose, the direction and the moving speed of the grinder were specified via a graphic interface on a screen. In total, the subject had to grind the pattern four times in a row without pausing. Thus, we achieved a total measurement time of 16 s, which corresponds to DIN EN ISO 28927-3 (28927-3:2010-0, 2010). Fig. 5 shows a picture of the graphical interface with the pattern the subject had to follow. Due to a defect in the random orbital sander, the number of subjects in the sanding task was only 26. The defective sander was replaced with a new one of the same model and manufacturer. In all three tasks of holding, pressing, and grinding, no force feedback was provided to achieve unaffected gripping behavior.

2.4. Analysis of the grip force and influence of the pressing force

a) General description of the method used

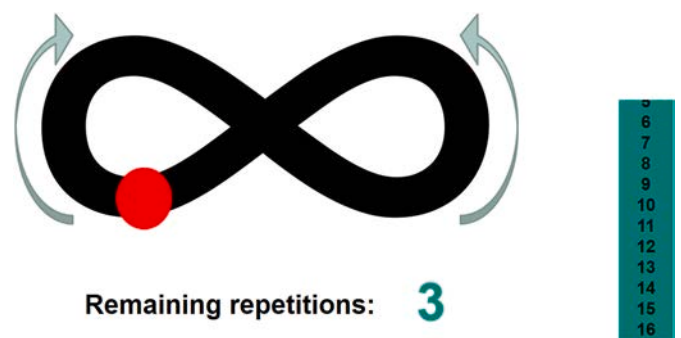


Fig. 5. Graphical surface of the pattern to be ground by the subject. The red dot shows the predefined position of the sander on the pattern. The green bar shows the remaining time of measurement. (For interpretation of the references to color in this figure legend, the reader is referred to the Web version of this article.)

To determine the grip forces, we used the 3D model of the grip obtained by 3D scanning of the grip geometry. The force values given by the sensor foil must be allocated and oriented to the 3D geometry of the handle. This is done by manually probing all sensor elements on the physical device and matching the location on the 3D scan. The spatial sensor element orientation is determined numerically from the scan geometry with the element direction being perpendicular to the handle surface. As a result of the above-mentioned step, each sensor element is assigned to a set of spatial coordinates and a normal vector in the 3D scan. An overview of the procedure is given in Fig. 6.

The procedure for finding a separation plane is based on (Schroder et al., 2020).

To find the optimal handle separation, two separate but analogous analyses were performed for each task of the study.

In order to find a three-dimensional representation of the handle separation, the problem is reduced to two-dimensional analyses. To do so, the 3D geometry and the force vectors from the sensor foil are projected onto the x-y and x-z planes, which represent the front and the top views of the handle. It should be mentioned that for projection in the x-z plane, the entire depth along the y-axis of the handle is taken into account. This means that the sensors of the force measurement foil, which are positioned on the curved surface below the top of the handle, are also projected in the x-z plane.

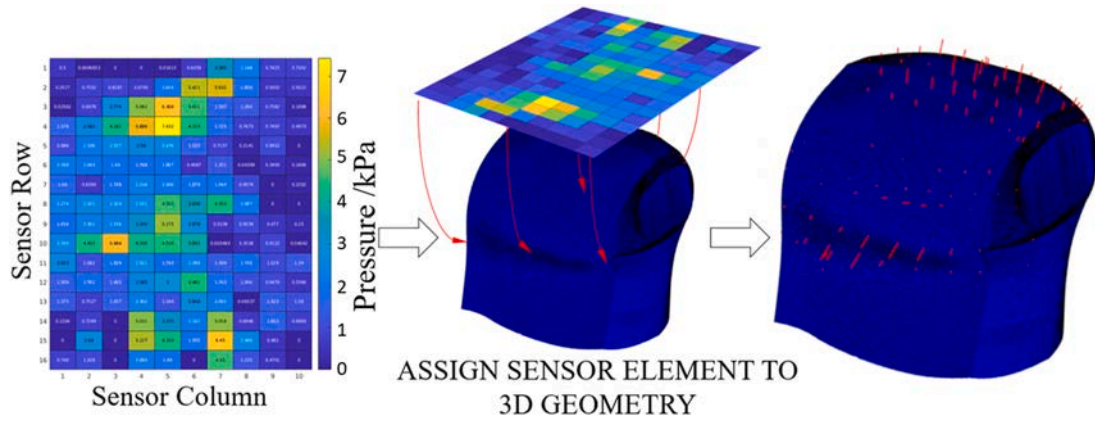


Fig. 6. Schematic presentation of the projection of the force measurement foil values onto the 3D model of the orbital sander handle. The left side of Fig. 6 shows the graphical representation of the sensor matrix of the force measurement foil. While each rectangle represents a sensor element, the colors characterize the pressure applied to the respective sensor element from blue (low pressure) to yellow (high pressure) (Schröder et al., 2020). (For interpretation of the references to color in this figure legend, the reader is referred to the Web version of this article.)

The angular position of the separation plane in the z-y plane is negligible, since the projections in the x-y and x-z planes cover any direction in which the vectors of the force sensors could potentially be oriented.

b) Detailed description of the mathematical model used for the determination of handle separation

The determination of the angular position of the separation plane

described below was performed in the same way for all three tasks.

The angular position of the separation plane in the x-y and x-z planes was determined separately here, but the same data evaluation method was used in both cases.

In a first step, the geometric center of all points to which the sensor elements are assigned is calculated. As depicted in Fig. 7, the reference coordinate systems $x-y$ and $x-z$ are placed in the geometric center O . In these initial reference frames, the edge of the separation plane is defined with an angle α relative to the vertical axis. The edge of the

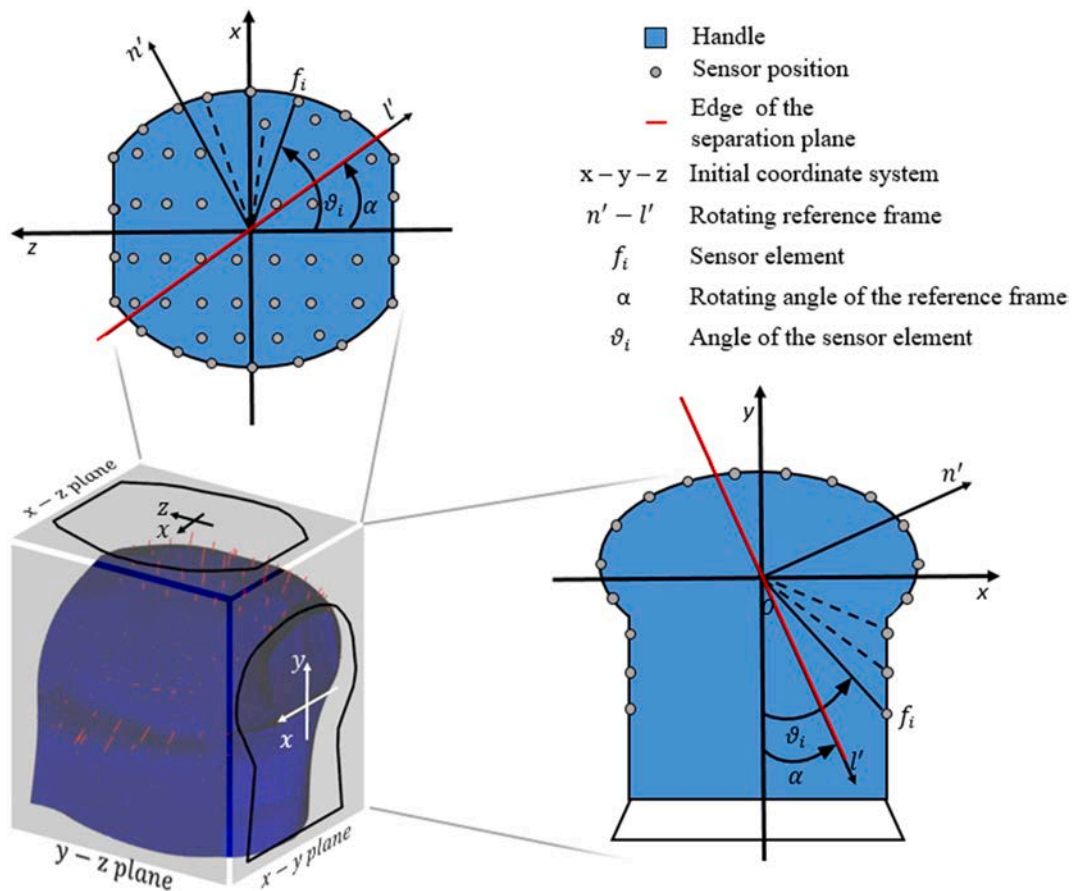


Fig. 7. Rotation of the reference frame $n' - l'$ by the angle $\alpha \in [0, \pi]$ in the x-y- and the x-z-planes of the initial coordinate system of the sander handle. The angle between the vertical y- or z-axis and the angular position of the specific sensor element f_i of the force measurement foil is given by ϑ_i .

separation plane is described by a rotating reference frame with a normal (n') and lateral direction (l').

For a given angle α , the sensor elements f_i are separated into two groups at the edge given by the angle α . Elements with a relative angle ϑ_i in the range $\alpha \leq \vartheta_i \leq \alpha + \pi$ are combined in the *A group*, while elements outside of this range are assigned to the *B group*. The normal vectors n_i of each sensor element f_i , are normally expressed in the global coordinate system. For the given angle α , these normal vectors n_i , are transformed to the reference frame ($n' - l'$).

$$\vec{n}_{i,(n' - l')} \begin{pmatrix} \sin\alpha & \cos\alpha \\ \cos\alpha & \sin\alpha \end{pmatrix} * \vec{n}_{i,(x - y)} \quad (1)$$

$$\vec{n}_{i,(n' - l')} \begin{pmatrix} \sin\alpha & \cos\alpha \\ \cos\alpha & \sin\alpha \end{pmatrix} * \vec{n}_{i,(x - z)}$$

For each angle α for $\alpha \in [0, \pi]$ in $n\alpha = \pi/180$, increments of the normal vectors are transformed to the rotated reference frame.

After transformation of the normal vectors for each angle $\alpha \in [0, \pi]$, the rotated normal vectors are fitted with the force measurement foil sensor data for each subject. This results in a course of the normal forces over the test duration projected onto the separation plane for each α .

To find the optimum separation angle α_{res} within the specific projection of the separation plane, all force vector components normal to the plane are added by

$$F_{res}(t, \alpha) = \sum_i f_i(t) \vec{n}_{i,(n' - l')}(\alpha) \cdot \vec{e}_{n'}(\alpha) \quad (2)$$

This step is done for the *A* and *B groups* separately. This results in a time course of the resulting force normal to the separation plane. The vector $\vec{e}_{n'}(\alpha)$ denotes the unit vector normal to the separation plane and (n) denotes the scalar product. The scalar product with $\vec{e}_{n'}(\alpha)$ ensures that only the part of $\vec{n}_{i,(n' - l')}(\alpha)$ which acts parallel to n' and normal to the separation plane is taken into account.

To find the optimal angular orientation of the separation plane, it is assumed that the time integral

$$I(\alpha) = \int F_{res}(t, \alpha) dt \quad (3)$$

is at its maximum at α_{opt} . Using Equations (2) and (3), the specific angle α_{opt} at which $I(\alpha)$ reaches its maximum is calculated for the *A* and *B groups* for each subject. The angle $\alpha_{opt A}$ is the angular orientation at which $I(\alpha)$ of the *A group* reaches its maximum on the separation plane. The angle $\alpha_{opt B}$ refers to the *B group* in the same way. The two angles $\alpha_{opt A}$ and $\alpha_{opt B}$ may deviate slightly from each other.

Referring to Equation (2), $I(\alpha)$ depends on two factors. The first factor is the measured value of each sensor element $f_i(t)$. The second factor is the amount of sensor elements belonging to the *A* or the *B group* for a specific rotation angle of the separation plane. The edge of the separation plane rotates in discrete steps with $\Delta\alpha = \pi/180$. Thus, belonging of a particular sensor element to the *A* or the *B group* may change within one increment step of $\Delta\alpha = \pi/180$. Therefore, the amount of sensor elements and hence $I(\alpha)$ of the *A* and $I(\alpha)$ of the *B group* varies for each α . This variation causes the deviation between $\alpha_{opt A}$ and $\alpha_{opt B}$. For these specific angles $\alpha_{opt A}$ and $\alpha_{opt B}$, the amount of sensor elements in the *A* and the *B groups* is slightly larger.

As the components of the grip force cancel each other out in the center of the palm, the value of $I(\alpha)$ from the *A* and *B groups* must be the same for a specific rotational angle α_{sep} of the separation plane's edge. Since the angle α_{sep} should also be the angle at which the maximum normal forces act on the separation plane, it has to be in the range of $\alpha_{opt A}$ and $\alpha_{opt B}$. Therefore, we calculated α_{sep} by the arithmetic mean of $\alpha_{opt A}$ and $\alpha_{opt B}$ for each subject. The result of this procedure is the edge of the separation plane in the x-y respectively x-z plane at the subject-specific angle $\alpha_{sep xy}$ respectively $\alpha_{sep xz}$. Fig. 8 shows the splitting of the sensor foil's sensors into the *A* and the *B group* for their projection in the x-y and the x-z planes. In addition, the figure shows the resulting angles $\alpha_{opt A}$ and $\alpha_{opt B}$ for the separation planes of both groups, where α_{sep} is located in between for both projections.

We subsequently calculated $\alpha_{res xy}$ and $\alpha_{res xz}$ as the median of $\alpha_{sep xy}$ and $\alpha_{sep xz}$ over all 30 subjects. Since this method was applied in the same way for all three tasks performed in the study, we obtained the angular orientation of the separation plane in the x-y and x-z projections. In the following, we calculated the arithmetic mean over the task-specific angles of $\alpha_{res xy}$ and $\alpha_{res xz}$ to obtain the angular orientation α_{xy} and α_{xz} of the resulting separation plane edges in each projection.

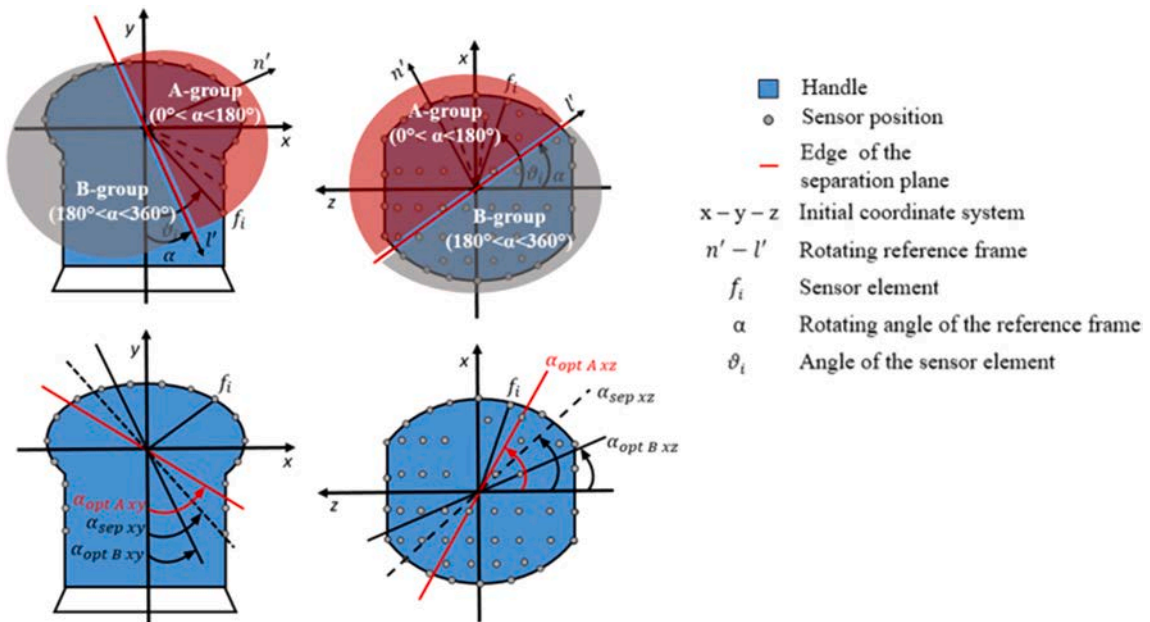


Fig. 8. Splitting of the sensors set into the *A* and *B group* (red and gray) exemplified for one subject with the resulting separation planes of each group oriented by $\alpha_{opt A}$ and $\alpha_{opt B}$ the intervening separation plane of α_{sep} for both projections. (For interpretation of the references to color in this figure legend, the reader is referred to the Web version of this article.)

The resulting two edges of the separation plane can be understood as two vectors spanning a separation plane which is defined by Equation 4:

$$x = y^* \sin(\alpha_{xy}) + z^* \sin(\alpha_{xz}) \quad (4)$$

c) Evaluation of the influencing factors in the determination of the separation plane.

In this chapter, we compared the resulting grip force of a separation plane oriented only by the angles $\alpha_{res\ xy}$ and $\alpha_{res\ xz}$ to a vertically oriented separation plane. This comparison was done to determine how the angular offset of the separation plane affects the resulting grip force. For this purpose, we calculated the resulting force vectors of the A and B groups for the separation plane oriented by α_{xy} and α_{xz} over all subjects for each task separately. For comparison, we calculated the resulting force vectors in the same way for the A and B groups in the case of a vertically oriented separation plane. Subsequently, the percentage deviation between the resulting forces from the A and B groups was calculated separately for the x-y and x-z projections using Equation (5).

$$D_{res\ xy/xz\ A/B} = 100 * \left| \left(1 - \frac{F_{res\ xy/xz\ A/B}(\alpha_{xy/xz})}{F_{res\ xy/xz\ A/B}(\alpha_{xy/xz})} \right) \right| \quad (5)$$

In Equation (5), $F_{res\ xy/xz\ A/B}(\alpha_{xy/xz})$ stands for the resultant grip forces acting normal to the determined separation plane. $F_{res\ xy/xz\ A/B}(\alpha_{xy/xz})$ was calculated separately for the A and the B groups and for the projections in the x-y and x-z planes. Consequently, $F_{res\ xy/xz\ A/B}$ stands for the corresponding resultant grip forces acting normal to a vertical separation plane and was calculated in the same manner. The specific percentage deviation between the resulting forces is also divided by group and projection plane and is indicated by $D_{res\ xy/xz\ A/B}$.

In addition to the deviation to a vertical plane, the influence of the pressing force on the angular alignment of the determined separation plane was also analyzed. In the pressing and grinding tasks, the gripping force distribution and thus the angular alignment of the separation plane can possibly be influenced by the pressing force exerted by the subject. Hence, we calculated the pressing force by summing all y-components of all vectors in both tasks. Since the upward and downward vectors of the grip force cancel each other out in this case, the result of this sum corresponds to the pressing force $F_{p\ res}$. This calculation was performed for each subject for the pressing and grinding tasks. The pressing force $F_{p\ res}$ was matched with the respective task specific angles $\alpha_{sep\ xy}$ of the separation plane individually for each task and subject. The pressing force $F_{p\ res}$ acts in negative y-direction, thus it can only influence the orientation of the separation plane in the x-y plane. The orientation in the x-z plane seen from above is not influenced, since the vector of the pressing force is directed into the viewing plane and cannot act on the projection of the separation plane.

Based on this subject-wise matching of $\alpha_{sep\ xy}$ and $F_{p\ res}$, we made a Spearman correlation analysis with the software SPSS. The Spearman correlation was used since the number of subjects performing the grinding task was less than 30 and we could not prove normal distributions for either the values of $F_{p\ res}$ or the values of $\alpha_{sep\ xy}$ using the Shapiro-Wilk test.

Table 3

Minimum, maximum, and the 5th and 95th percentile of the subject-specific separation planes' orientations in the x-y plane over all three tasks performed in the study.

	Holding [°]	Pressing [°]	Grinding [°]
Minimum	-15	-17.5	-14
Maximum	2	4.5	2
Median ($\alpha_{res\ xy}$)	-7	-0.25	-2.5
5th percentile	-13	-15.5	-13.62
95th percentile	1.5	4	1.25

3. Results

3.1. Determination of the separation plane

The first part of the results chapter showcases the angular orientation of the separation plane's edge in the x-y-plane and x-z plane for the different tasks. Following from this, the three-dimensional orientation of the separation will be shown at the end of the results chapter. Table 3 shows the task-related distribution of $\alpha_{sep\ xy}$ over all subjects. Hereby Table 3 lists the minimum, maximum and median angle $\alpha_{res\ xy}$ as well as the percentiles.

Regarding the minimum and maximum values and the percentiles of Table 3, it can be seen that the separation planes' edges are oriented in the same range over all tasks performed. The values of Table 3 show that the angles of the separation planes in the x-y plane are slightly shifted into the negative range, as the absolute value of the minimum is larger than the absolute value of the maximum, which is consistent with the values of the 95th and 5th percentiles. Fig. 9 shows, a projection in the x-y plane of the task-specific separation plane edges, which are specifically oriented through their resulting median angle $\alpha_{res\ xy}$.

The edges are represented as lines in the x-y projection of the sensor positions of the force measurement foil with the geometric center 0' being the center of rotation. Through the orientation of the position vectors of sensors from the force measuring foil shown in blue, the shape of the orbital sander handle in the x-y plane is apparent. Therefore, it can be concluded that the foil was correctly positioned on the orbital sander handle.

The edges of the resulting separation planes shown in Fig. 9 are nearly vertical, as the values of the median respectively $\alpha_{res\ xy}$ from Table 3 are close to zero. In particular, the planes' edges of the grinding and pressing tasks are very close to the vertical with a value of $\alpha_{res\ xy}$

0.25°, the edge resulting from the pressing task is almost vertical. The plane's edge from the holding task has an angle of $\alpha_{res\ xy} = 7^\circ$, which deviates from the two other angles. This is also visible in Fig. 9, since the gap between the line of the holding task and the two others is larger than their gap to each other.

Following Fig. 9, Table 4 shows the task-related distribution of $\alpha_{sep\ xz}$ over all subjects. As for the resulting angles of $\alpha_{sep\ xy}$ in the x-y plane, the minimum, maximum, and median values and the 5th and 95th percentiles are given.

According to Table 4, the separation plane edges in the x-z plane tend to be vertically oriented with a slight shift to the negative. For the percentiles of Table 4, a slight shift of $\alpha_{sep\ xz}$ into the negative range as in the case of $\alpha_{sep\ xy}$ can be seen. This is visible by the absolute values of the 5th percentiles of all tasks being larger than the corresponding absolute values of the 95th percentiles. In this context it can be assumed that the maximum value of 9° the pressing task in Table 4, refers to the outlier, since it is much bigger than the 95th percentile. Consequently the median angles of the respective tasks in Table 4 also deviate slightly from the vertical into the negative and are very close to each other. In the following, Fig. 10 presents the separation planes' edges of each task oriented by the median angle $\alpha_{res\ xz}$, which represents the angular orientation of the separation plane in the top view of the handle. Since the whole top side of the handle is covered with the measurement foil, the sensor positions are distributed all over the plot as shown in Fig. 10. From the shape of this blue dotted cloud, it is possible to guess the shape of the handle of the random orbital sander viewed from above. Therefore, it can be assumed that positioning of the force measurement foil and the calculation of the sensor positions on the handle were correct.

As expected from the values of the median angles $\alpha_{res\ xz}$ in Table 4, the task-specific separation plane edges in Fig. 10 lie nearly on top of each other with a slight angular offset of minus five degrees from the vertical. With the angular orientations of the separation planes' edges in the x-y and x-z planes from Figs. 9 and 10, a three-dimensional representation of each separation plane can be calculated by using Equation

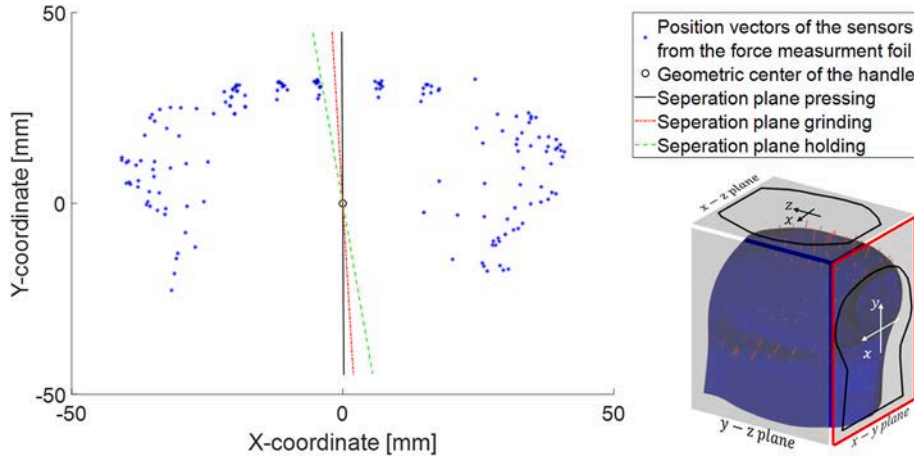


Fig. 9. Resulting angular orientation $\alpha_{res\ xy}$ of the separation plane's edge in the x-y plane for all three tasks performed.

Table 4

Minimum, maximum, median, and the 5th and 95th percentile of the subject-specific separation planes' orientations in the x-z plane over all three tasks performed in the study.

	Holding [°]	Pressing [°]	Grinding [°]
Minimum	-22	-14	-30.5
Maximum	7	9	4
Median ($\alpha_{res\ xz}$)	-6	-5.75	-4.75
5th percentile	-15	-14	-13.5
95th percentile	6.5	0.5	0.5

(4). Based on these three task specific separation planes the total separation plane over all three tasks performed was determined. Therefore the arithmetic mean angle of $\alpha_{res\ xy}$ and $\alpha_{res\ xz}$ over all tasks was calculated. The angular orientation of this total separation plane is given by $\alpha_{mean\ xy}$ 3.25° and $\alpha_{mean\ xz}$ 5.5°. A three-dimensional representation of the task specific separation planes passing through the sander's handle as well as a three-dimensional representation of the calculated total separation plane can be found in the appendix of the manuscript.

3.2. Influence of the pressing force and deviation to the vertical

The second part of the results chapter shows the percentage deviation of the grip force with respect to the calculated separation plane compared to a fully vertical separation plane. In addition, the influence of the pressing force on the angular orientation of the separation plane will be presented.

The separation planes' orientations in the x-y and x-z planes are approximately vertically across all tasks.

Therefore, it has to be evaluated whether a vertically oriented separation plane respectively a vertical splitting of the measurement handle is sufficient. Under the conditions of an easy-to-manufacture design, a vertically oriented splitting of the measurement handle would be less expensive and easier to manufacture. Thus, Table 5 shows the maximum, the minimum, and the median value of the deviations $D_{res\ xy-A/B}$ and $D_{res\ xz-A/B}$ between the resulting grip force for the task-specific determined separation plane and a vertically oriented separation plane. These characteristic values of $D_{res\ xy-A/B}$ and $D_{res\ xz-A/B}$ are divided into those of the x-y and x-z projections to allow separate evaluation. Furthermore, the values are divided into the *A* and *B* groups. This is due to the fact, that the components of the grip force cancel each other out in the center of the palm. Therefore, the resulting grip force of

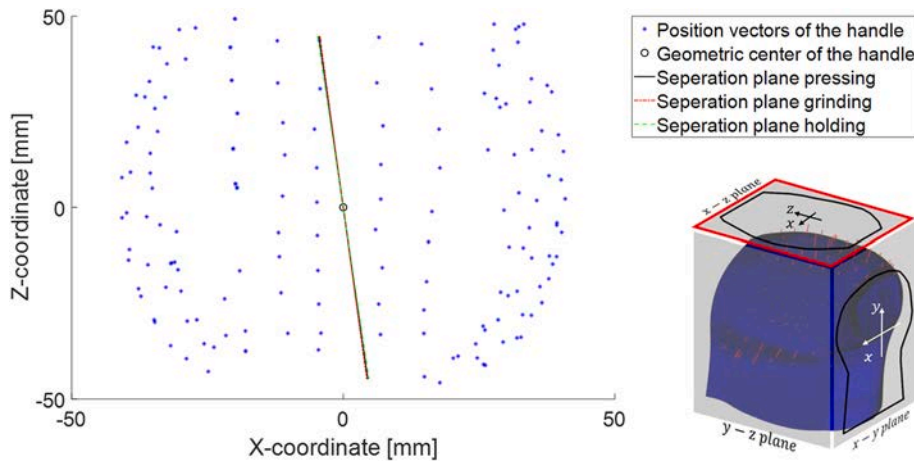


Fig. 10. Resulting angular orientation $\alpha_{res\ xz}$ of the separation plane's edge in the x-z plane for all three tasks performed.

Table 5

The minimum, maximum, and mean values of the percentage deviations between the resulting grip force acting on the separation plane oriented by α_{sep} and the one acting on the vertically oriented separation plane. The deviation is calculated separately for the corresponding planes α_{sep_xy} and α_{sep_xz} in the x-y and x-z planes.

			Holding task [%]	Pressing task [%]	Grinding task [%]
x-y plane	A group	Minimum $D_{res_xy_A}$	0.40	0.00	0.01
		Maximum $D_{res_xy_A}$	2.10	0.07	0.75
		Median $D_{res_xy_A}$	1.30	0.02	0.23
	B group	Minimum $D_{res_xy_B}$	0.03	0.06	0.3
		Maximum $D_{res_xy_B}$	1.20	0.18	1.30
		Median $D_{res_xy_B}$	0.45	0.10	0.92
x-z plane	A group	Minimum $D_{res_xz_A}$	0.13	0.09	0.49
		Maximum $D_{res_xz_A}$	8.73	5.20	7.09
		Median $D_{res_xz_A}$	1.96	1.59	2.66
	B group	Minimum $D_{res_xz_B}$	0.17	0.34	0.00
		Maximum $D_{res_xz_B}$	8.33	6.50	8.30
		Median $D_{res_xz_B}$	2.18	3.00	2.64

each subject for each task and the percentage deviation were calculated separately for both groups. The percentage deviation between the resulting grip force acting on the determined separation planes and the one acting on a vertical separation plane is overall below 10%. Furthermore, this deviation is smaller in the x-y plane than in the x-z plane across all tasks. Regarding the different tasks, it can be seen that the resulting grip force from the pressing task has the smallest percentage deviation compared to the resulting grip force that would act on a vertical separation plane. This trend is visible for the values of both groups and for both projections, except for the minimum value of the *B group* which is the largest in both projections compared to that of the other tasks. Defining the range of the percentage deviation as the range between the minimum and the maximum value, Table 5 shows that this range is the largest for the holding task and the smallest for the pressing task. This observation can be made across all tasks and projections except of the *B group* in the x-z plane where the range of the grinding task is slightly larger.

To determine the influence of the pressing force F_{p_res} on the separation planes' angular orientation α_{res_xy} in the x-y plane, a Spearman correlation analyses was carried out. The results of this analysis indicate a significant correlation of $p = 0.03$ between the pressing force and the angular orientation of the separation plane of the pressing task (The correlation is significant at the 0.05 level (two-sided)). In the case of the grinding task, no significant correlation between the pressing force and the angular orientation of the separation plane could be detected. Regarding the effect size of F_{p_res} on α_{res_xy} for the pressing task, a value of $r = 0.4$ indicates a medium effect.

4. Discussion

4.1. Splitting of the knob-shaped measuring handle

With the method used, it was possible to extract design parameters for a knob-shaped measurement handle from the experimental data of a subject study using a numeric algorithm. Based on the results obtained, the first main question of the manuscript concerning the angular orientation of the separation plane in the knob-shaped handle will be discussed and compared to the cylindrical measurement handle.

Across all tasks performed and subjects participating, the results show that the separation plane for a knob-shaped handle is predominantly vertically oriented with an overall orientation $\alpha_{mean_xy} = 3.25^\circ$ and $\alpha_{mean_xz} = 5.5^\circ$. This angular orientation of the separation plane shows that the grip force on a knob-shaped handle acts predominantly

horizontally.

In this case, the alignment of the separation plane to the pressing force and to the respective power tool movement deviates from the established cylinder handle. With the cylindrical handle, the separation plane is perpendicular to the pressing force and to the axis of the forearm and the direction of a representative power tool movement. In contrast to this, the separation plane of the knob-shaped handle is oriented parallel to the direction of the pressing force and to the axis of the forearm.

Hence, for a knob-shaped handle, the relations between coupling forces and power tool movements are more complex than in the case of power tools with a mainly cylindrical handle such as the hammer drill. The power tool movement of the orbital sander is planar, while the pressing force is perpendicular to this movement as it presses the grinding disc against the surface of the plywood plate. Moreover, the grip force is perpendicular to the pressing force and mostly independent of the power tool movement. Evidence of this independence is provided by the values in Tables 4 and 5, where the 5th and 95th percentiles of the grinding and static pressing tasks are in the same range. In addition, the 95th and 5th percentiles of both projections range from 15.5° to 6.5° across all tasks, which is consistent with a separation plane that is slightly negative to the vertical.

The scatter of the individual separation planes, which can be seen by the percentiles in Tables 4 and 5 may be due to the scatter of the subjects' hand and finger sizes shown in Table 2. The scatter may also be due to the shape of the grip. Compared to the unidirectional gripping of a cylindrical handle or a power grip, the knob-shaped handle allows more flexible positioning of the palm and fingers on the handle surface. This may lead to a higher variability of the gripping position across the subjects.

4.2. Influence of subjects' handedness and the applied pressing force

Regarding the separation planes in Figs. 9 and 10, it has to be mentioned that in all tasks, the planes are slightly shifted negative to the vertical. This negative angular offset from the vertical is also evident from the values of α_{res_xy} and α_{res_xz} in Tables 4 and 5. In the x-z plane, this negative angular offset has a similar magnitude in all tasks in the range of 5.5° as is shown in Fig. 10, where the separation planes are oriented almost on top of each other. In the x-y plane, the separation planes of the different tasks differ more from each other. While the negative offset to the vertical in the holding task is about the same in the x-y and x-z planes, the separation planes of the pressing and the grinding tasks are

oriented clearly more vertically in the x-y plane than in the x-z plane.

Overall, the negative angular offset is more pronounced in the x-z plane, firstly, because it is approximately the same for all three tasks, and secondly, because on average, it is greater than the offset in the x-y plane. Accordingly, it can be assumed that the offset has the same cause in all three tasks.

A possible explanation of the negative angular offset in the x-z plane could be that the subjects in the study were only right-handed. In the case of a knob-shaped handle, the subject's hand is mounted on the top of the handle and the arm is oriented backwards to the handle as an extension of the palm. Therefore, the subject must rotate the hand slightly so that the index finger is on the front of the handle, while the thumb and other fingers are on either side of the knob-shaped handle, facing each other. Such way of gripping can be seen in Fig. 4, a similar type of gripping is also described in (Wakula et al., 2009). In this type of gripping, the grip axis of the thumb and fingers runs diagonally across the palm from the index finger to the wrist. For a right-handed person, this diagonal gripping axis has a negative angular offset because, from the user's point of view, the gripping axis runs from the left front side to the right rear side of the orbital sander handle. With reference to the results in Table 4 and Fig. 10, the angular offset of the separation planes from the vertical in the x-z plane would correspond to the gripping axis of a right-handed subject. Therefore, the connection between the angular offset of the separation plane in the x-z-plane and the only right-handed subjects of the study is a reasonable assumption.

According to this assumption, the angular offsets in the x-y plane must also be discussed. In the x-y plane, the assumed influence of the subjects' right-handedness only affects the separation plane of the holding task, whose angular orientation $\alpha_{res\ xy}$ is nearly the same as in the x-z plane, as is shown in Tables 4 and 5. In contrast, Fig. 9 and the values of $\alpha_{res\ xy}$ in Table 3 show that the separation planes of the pressing and grinding tasks are oriented approximately vertically in the x-y plane. A possible explanation for these differences in the x-y plane is that no pressing force was applied to the random orbital sander during the holding task. The grip force could thus act uninfluenced on the sander without being stabilized by being pressed against the plywood. This uninfluenced acting of the grip force leads to a stronger effect of the right-handedness of the subjects in the holding task. This explanation is supported by the similar angular orientations of the different separation planes in the x-z plane in Fig. 10 and Table 4. Since the vector of the pressing force is directed downward into the x-z plane, it cannot act normally on the projection of the separation plane and does not contribute to its orientation. Therefore, the separation planes' orientations in the x-z plane are only influenced by the grip force. In consequence, the separation planes of the pressing and grinding tasks are oriented in a similar angle as the separation plane from the holding task. In the x-y plane, on the other hand, the applied pressing force causes the separation planes of the pressing and grinding tasks to be more vertically aligned, while the separation plane of the holding task has a similar angle as in the x-z plane, since no pressing force was applied. In the case of the pressing task, this explanation is supported by the results of the Spearman correlation analyses, which show a medium effect size for a significant correlation between $\alpha_{res\ xy}$ and the resulting pressing force $F_{p\ res}$. In the case of the grinding task, no significant correlation could be shown. The fact that no significant correlation between $\alpha_{res\ xy}$ and the resulting pressing force $F_{p\ res}$ could be shown for the grinding task may be due to the task itself and the corresponding test procedure. In the pressing task, the subjects only had to apply static force to the sander while in the grinding task, the sander was moved. In consequence, the subjects had to apply less pressing force in the grinding task. Furthermore, in the pressing task, the subjects were instructed to press

the random orbital sander against the plywood plate. This instruction can lead to a more intentional application of the pressing force, as the subjects only had to pay attention to it. In the grinding task, the subjects had to pay attention to the grinding of the pattern, hence they possibly paid less attention to the application of the pressing force. In consequence, no correlation between the applied pressing force in the grinding task and the specific angle of the separation plane in the x-y plane could be shown. A possible indication of this assumption could be that the pressing force of the grinding task is not normally distributed across the subjects.

To answer the second main question of the manuscript, the results show that in the pressing task, the applied pressing force reduces the value of $\alpha_{res\ xy}$ to a more vertical orientation of the separation plane in the x-y plane. Hereby, the assumed effect of the subjects' right-handedness is compensated. A similar effect can be assumed for the grinding task, but could not be proven by the correlation analyses, which is probably due to the test procedure. In further studies, this assumption had to be analyzed. A possible test procedure for this would be to give the subjects several different values for the pressing force during the grinding task. Regarding the assumed effect of right-handedness, it would be interesting to also consider left-handed subjects in the study, since a shift of $\alpha_{res\ xy}$ to the positive would be expected.

4.3. Design and implementation of the knob-shaped measuring handle

Based on the results obtained concerning the orientation of the separation plane and the influence of the pressing force, it has to be evaluated how the splitting of the knob-shaped measurement handle has to be implemented.

Assuming a negative separation plane shift for right-handers and a positive shift for left-handers, a vertical splitting of the knob-shaped measuring handle would be a possible suitable design, as it would be suitable for both right- and left-handers.

Considering the effect of the pressing force on the separation plane orientation in the x-y plane, a vertical splitting of the knob-shaped measuring handle would also make sense. Based on the results obtained, it can be assumed that the application of the pressing force causes a rather vertical alignment of the separation plane. Since the pressing force is also applied during the impedance measurement on shaker-based test benches, a vertical splitting of the handle would be a reasonable option. Therefore, it has to be evaluated how much a vertical splitting of the knob-shaped measurement handle would influence the resulting grip force. The results of the percentage deviation between the pressing forces acting on the determined and on the vertical separation plane in Table 5 are overall below 10% including both projections, all tasks, and both groups. In this context, it can be seen that the values of the maximum and median percentage deviation in the x-z plane are greater than in the x-y plane across all tasks. This trend corresponds to the separation plane angles in Figs. 9 and 10, where the angular deviation from the vertical in the x-z plane is also greater than in the x-y plane across all tasks. Furthermore, Table 5 shows that the percentage deviation of the grip force is lowest for the pressing task, especially as far as the deviation in the x-y plane is concerned. This deviation also coincides with the alignment of the separation plane of the pressing task, as this has the smallest angular deviation from the vertical. With regard to the intended use of the measuring handle, this is most likely represented by the pressing task. Following on from this, the maximum percentage deviation between the gripping forces applied to the different separation planes is lowest for the pressing task in both projections. If one also takes into account that the measuring handle should be suitable for right- and left-handed subjects, a vertical splitting of the measuring

handle would be an acceptable and easy-to-manufacture design.

5. Limitations

The results of the study only refer to one specific random orbital sander. Although the analyzed gripping position is representative of this type of sander, the results obtained are limited to the specific geometry of the sander handle. Since this geometry may vary slightly for a different random orbital sander, different results are possible. With a wider handle, the fingers of the subject's hand would close less around the handle and rest more on the top than on the side of the handle. In this case, the applied grip force would act more vertically than horizontally. The subjects' grip force could also be affected by the thickness of the force measurement foil as it increases the dimensions of the handle. Since the foil's measurement works by compressing a layer of elastomer, a certain thickness is required for the measurement. For determination of the separation plane, the foil's sensor elements were evaluated relative to each other. The influence of the film thickness on the angular position of the separation plane can thus be considered minor, since it affects all sensors and the grip force distribution of all subjects in the same way.

In this context, it also has to be considered that the height of the plywood plate was fixed, which caused variations in the arm posture depending on the standing height of the subject. For tall subjects, a plywood plate that is too low could possibly cause the subjects to bend over the plywood plate more and add parts of their body weight to the pressing force. Considering the correlation between the subject's handedness, the separation plane's angular orientation, and the pressing force derived from the results obtained, the resulting higher pressing force would lead to a more vertical separation plane. Conversely, a plywood plate that is too high would result in small subjects applying less pressing force as they would not be able to align their arms properly, resulting in a less vertical separation plane. With regard to the study carried out, these correlations have probably influenced the obtained alignments of the separation planes' orientation, but the height of the subjects was predominantly in a relatively small range between 1.70 m and 1.90 m (23 out of 30 subjects). Therefore, the influence of the varying standing height of the subjects on the results obtained may be less than would be the case if the height of the subjects was normally distributed. Consequently, in further studies, the height of the plywood plate must be adjusted to the scatter of the subjects' body size.

Furthermore, only right-handed subjects were considered in this study. It would be wise to include left-handed subjects as well. In this context, the obtained results of the study are also limited by the scatter of the calculated individual subject-specific separation planes. This scatter is possibly caused by the different hand sizes of the subjects. Therefore, further studies using the same method of evaluation are required, since the subjects of the conducted study were only right-handed and not normally distributed in their anthropometric properties. Hereby, the study focused on the direction and orientation of the subjects' grip forces. Therefore, the force distribution across the handle was more relevant than the absolute value of the applied grip force. In consequence, the measurement of the subjects' anthropometric properties included only the hand dimensions according to DIN EN ISO 7250-1, since the dimensions and kinematics of the hand are related to the force distribution on the handle. The muscle strength and capacity play a minor role in determining this force distribution, therefore specific measurement of the subject's muscle strength was not necessarily required. However, it would be interesting to measure the muscle strength of the subjects in further studies, as it cannot be assumed that it is the same over all subjects. In this regard, measuring the subject's maximum voluntary isometric contraction (MVIC) would be a good

indicator for the subject's muscle strength (Meldrum et al., 2007). In addition the data analyses could be combined with the ability of the novel force measurement foil to segment its force sensors. This segmentation sums up the applied force of a defined amount of sensors located in a certain area to one total value. Implementing this ability into the evaluation algorithm could possibly reduce the effort of assigning the sensor positions to the 3D scan and lower the computing time. Through this optimization, a greater amount of handles could be evaluated faster.

Furthermore, the subjects' experience in the use of power tools considered only the use in general and did not refer to specific power tools. A possible connection between the angular orientations of the separation planes and the subjects' explicit power tool experience was not analyzed.

Nevertheless, further studies are required to analyze the relationship between the subjects' experience in handling certain power tools and the forces applied to these power tools. Therefore, the subjects' performance of a specific task related to one power tool would be a possible appropriate test setup. Hereby, not only the grip force and its distribution, but also the pressing force and the movement of the power tool have to be recorded. In this context, a more specific query on the subjects' experience in handling power tools is necessary, as there are large differences in the use of certain power tools.

Conclusion

The manuscript introduces a novel approach to the data-based design of a new knob-shaped measuring handle for the measurement of grip force in the context of impedance measurement. Since no comparable design of a measuring grip exists according to the current state of research, the significant design parameters for a knob-shaped measuring handle were extracted from the data of a subject study. The subject study was conducted with 26 subjects whose gripping force on a random orbital sander was measured during various tasks performed. Based on the results of the study, a separation plane was calculated to divide the new knob-shaped measuring handle in order to integrate the force sensors for grip force measurement. The force sensors of the knob-shaped measuring handle have to be placed in a vertically oriented separation plane, since the grip force of the test subjects acts mainly horizontally on the sander handle. The separation plane shows a slight angular offset to the vertical, which may be due to the handedness of the subjects, since only right-handed subjects participated in the study. This angular offset caused by the handedness seems to be reduced by the pressing force.

In future studies, the approach has to be validated with different knob-shaped handles both for right- and left-handed subjects.

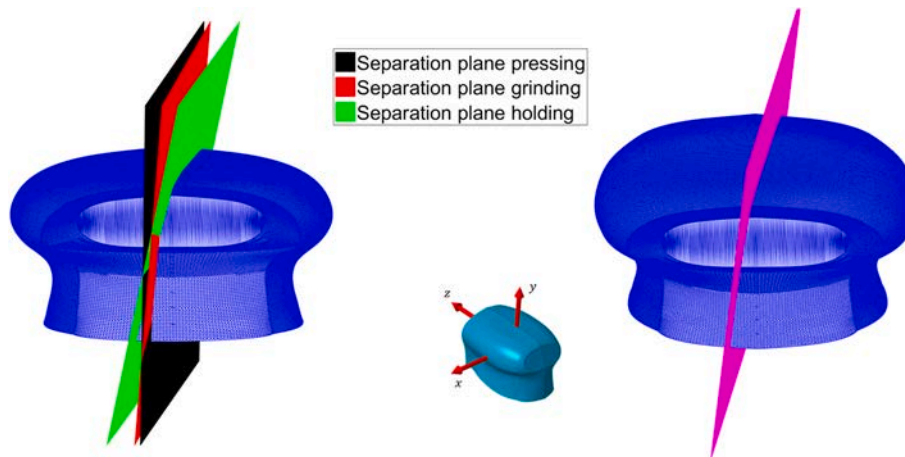
Declaration of competing interest

The authors declare that they have no known competing financial interests or personal relationships that could have appeared to influence the work reported in this paper.

Acknowledgement

This work was supported by the German research foundation Deutsche Forschungsgemeinschaft (DFG) under the funding number 408254169. The authors of this publication are responsible for its content. We want to thank the DFG for funding and the support of our research, which enabled this publication. We would like to emphasize that the presented results and conclusions do not necessarily reflect the opinion of the DFG.

Appendix A. 3D-representation of the mean separation plane for each task passing through the 3D-scan of the orbital sander's handle (left side). Overall separation plane calculated by the arithmetic mean over all three tasks



References

10819:2019-5; 2019DIN EN ISO 10819:2019-5, May. 2019. Mechanische Schwingungen und Stöße – Hand-Arm-Schwingungen – Messung und Bewertung der Schwingungsübertragung von Handschuhen in der Handfläche: Mechanical vibration and shock - Hand-arm vibration - Measurement and evaluation of glove palm vibration transmission. DIN Deutsches Institut für Normung e. V., Berlin, 10819.

28927-3:2010-0, 2010Handgehaltene motorbetriebene Maschinen - Messverfahren zur Ermittlung der Schwingungsemission Teil 3: Poliermaschinen sowie Rotationsschleifer, Schwingschleifer und Exzentrerschleifer (ISO 28927-3:2009): [Hand-held portable power tools –Test DIN EN ISO 28927-3:2010-05, May. 2010. Methods for Evaluation of Vibration Emission – Part 3: Polishers and Rotary, Orbital and Random Orbital Sanders, ISO 28927-3:2009], 28927-3. DIN Deutsches Institut für Normung e. V., Berlin.

DIN EN ISO 5349-1:2001, 2001. Mechanical Vibration – Measurement and Evaluation of Human Exposure to Hand-Transmitted Vibration – Part 1: General Requirements, ISO 5349-1:2001, ISO - International Organization for Standardization [Online]. Available: https://www.jstage.jst.go.jp/article/indhealth/43/3/43_3_485/_pdf/-char/ja.

DIN EN ISO 7250-1:2017: Wesentliche Maße des menschlichen Körpers für die technische Gestaltung – Teil 1: Körpermaßdefinitionen und -messpunkte: Basic human body measurements for technological design – Part 1: Body measurement definitions and landmarks, 7250-1, Dec. 2017. DIN - Deutsches Institut für Normung, Berlin.

Adewusi, S.A., Rakheja, S., Marcotte, P., Boutin, J., 2010. "Vibration transmissibility characteristics of the human hand–arm system under different postures, hand forces and excitation levels. *Journal of Sound and Vibration* 329 (14), 2953–2971. <https://doi.org/10.1016/j.jsv.2010.02.001>.

Aldien, Y., Marcotte, P., Rakheja, S., Boileau, P.-É., 2005a. "Mechanical impedance and absorbed power of hand- arm under xh–Axis vibration and role of hand forces and posture. *Industrial Health* 43, 495–508, 2005.

Aldien, Y., Welcome, D., Rakheja, S., Dong, R., Boileau, P.-E., 2005b. "Contact pressure distribution at hand–handle interface: role of hand forces and handle size. *International Journal of Industrial Ergonomics* 35 (3), 267–286. <https://doi.org/10.1016/j.ergon.2004.09.005>.

Bovenzi, M., 1994. Hand-arm vibration syndrome and dose-response relation for vibration induced white finger among quarry drillers and stonemasons. *Italian Study Group on Physical Hazards in the Stone Industry, Occupational and Environmental Medicine* 51 (9), 603–611. <https://doi.org/10.1136/oem.51.9.603>.

Burstrom, L., 1997. The influence of biodynamic factors on impedance of the hand and arm. *International Arch Occup Environ Health* (69), 437–446. <https://doi.org/10.1007/s004200050172>, 1997.

Dong, R.G., Rakheja, S., Schopper, A.W., Han, B., Smutz, W.P., 2001. Hand-transmitted vibration and biodynamic response of the human hand-arm: a critical review. *Critical Reviews in Biomedical Engineering* 29 (4), 393–439. <https://doi.org/10.1615/critrevbiomedeng.v29.i4.20>.

Dong, R.G., Wu, J.Z., Welcome, D.E., 2005. Recent advances in biodynamics of human hand-arm system. *Industrial Health* 43 (3), 449–471. <https://doi.org/10.2486/indhealth.43.449>.

Dong, R.G., Welcome, D.E., McDowell, T.W., Wu, J.Z., 2006a. Measurement of biodynamic response of human hand-arm system. *Journal of Sound and Vibration* 294 (4), 807–827. <https://doi.org/10.1016/j.jsv.2005.12.047>.

Dong, R.G., Welcome, D.E., McCormick, R.E., 2006b. 3-D laboratory simulation of hand-transmitted vibration in *Conference Proceedings of the Society for Experimental Mechanics Series*.

Dong, R.G., Welcome, D.E., McDowell, T.W., Wu, J.Z., 2013. Modeling of the biodynamic responses distributed at the fingers and palm of the hand in three orthogonal directions. *Journal of Sound and Vibration* 332 (4), 1125–1140. <https://doi.org/10.1016/j.jsv.2012.10.003>.

Dong, R.G., et al., 2012. Mechanical impedances distributed at the fingers and palm of the human hand in three orthogonal directions. *Journal of Sound and Vibration* 331 (5), 1191–1206. <https://doi.org/10.1016/j.jsv.2011.10.015>.

Edwards, D.J., Rillie, I., Chileshe, N., Lai, J., Hosseini, M.R., 2020. "A field survey of hand–arm vibration exposure in the UK utilities sector," *Engineering, Construction and Architectural Management* 27 (9), 2179–2198. <https://doi.org/10.1108/ECAM-09-2019-0518>.

Griffin, M.J., 1996. *Handbook of Human Vibration*, first ed. Academic Press, London, San Diego.

Hussein, N.I.S., Shukur, A., Kamat, S.R., Yuniawan, D., 2019. The impact of worker experience and health level to vibration absorbed by hand. *Journal of Advanced Manufacturing Technology (JAMT)*. <https://doi.org/10.1080/10937404.2018.1557576>, 2019.

VDI 2057 Blatt 2: *Einwirkung mechanischer Schwingungen auf den Menschen: Hand-Arm-Schwingungen: Effect of mechanical vibrations on humans: Hand-arm vibrations*, 2057 Blatt 2, 2016. VDI Verein deutscher Ingenieure e.V., Berlin, Mar.

Kalra, M., Rakheja, S., Marcotte, P., Dewangan, K.N., Adewusi, S., 2015. Measurement of coupling forces at the power tool handle-hand interface. *International Journal of Industrial Ergonomics* 50, 105–120. <https://doi.org/10.1016/j.ergon.2015.09.013>.

Kaulbars, U., 2006. Schwingungen fest im Griff: [Vibrations firmly under control (author's transl.)]. Technische Überwachung Düsseldorf 47 (6), 35–40 [Online]. Available: https://www.dguv.de/medien/ifa/de/pub/grl/pdf/2006_081.pdf.

Kaulbars, U., Lemerle, P., 2002. "Messung der Ankopplungskräfte zur Beurteilung der Hand-Arm-Schwingungen–Weiterentwicklung eines Messsystems: [Measurement of coupling forces for the evaluation of hand-arm vibrations-Further development of a measurement system (author's transl.)]. VDI-Berichte 99–111, 2007.

Kihlberg, S., Hagberg, M., 1997. "Hand-arm symptoms related to impact and nonimpact hand-held power tools," (in En;en). *Int Arch Occup Environ Health* 69 (4), 282–288. <https://doi.org/10.1007/s004200050148>.

Krajnak, K., 2018. Health effects associated with occupational exposure to hand-arm or whole body vibration. *Journal of toxicology and environmental health* 21 (5), 320–334. <https://doi.org/10.1080/10937404.2018.1557576>.

Lindenmann, A., Matthesen, S., 2019. The rotational mechanical impedance of the hand-arm system: a preliminary study. In *14th International Conference on Hand Arm Vibration. -Abstracts-*, Bonn, pp. 75–76.

Makita Werkzeug GmbH, DBO180Z - Akku-Exzentrerschleifer Datenblatt. [Online]. Available: <https://www.makita.de/product/dbo180z.html> (accessed: Jan. 22 2021.493Z).

Marcotte, P., Aldien, Y., Boileau, P.-É., Rakheja, S., Boutin, J., 2005. Effect of handle size and hand-handle contact force on the biodynamic response of the hand-arm system under zh-axis vibration. *Journal of Sound and Vibration* 283 (3–5), 1071–1091. <https://doi.org/10.1016/j.jsv.2004.06.007>.

Matthesen, S., Uhl, M., 2017. "Methodical approach for the analysis of the active user behavior during the usage of power tools," in *Design for X: beitrage zum 28. DFX-Symposium Oktober*, pp. 1–12, 2017.

Matthesen, S., Mangold, S., Bruchmüller, T., Marko, A.-M., 2014. "Der Mensch als zentrales Teilsystem in Wechselwirkung mit handgehaltenen Geräten – Ein

- problemorientierter Ansatz zur Untersuchung dieser Schnittstelle," in *Design for X: Beiträge zum 25. Oktober. DFX-Symposium, Bamberg*, pp. 193–204, 2014.
- Matthiesen, S., Lindenmann, A., Bruchmueller, T., 2018. "Anforderungen an ein Messsystem zur Ermittlung der Rotationsimpedanz von Hand-Arm Systemen," in 7. VDI-Tagung Humanschwingungen 2018, Würzburg, pp. 91–106.
- Matysek, M., Kern, T.A., 2009. *Entwicklung Haptischer Geräte: Ein Einstieg für Ingenieure*. Springer Berlin Heidelberg, Berlin, Heidelberg.
- Meldrum, D., Cahalane, E., Conroy, R., Fitzgerald, D., Hardiman, O., 2007. "Maximum voluntary isometric contraction: reference values and clinical application," *Amyotrophic lateral sclerosis*, 8 (1), 47–55. <https://doi.org/10.1080/17482960601012491> official publication of the World Federation of Neurology Research Group on Motor Neuron Diseases.
- DIN 45679:2013-02, 2013. *Mechanische Schwingungen - Messung und Bewertung der Ankopplungskräfte zur Beurteilung der Schwingungsbelastung des Hand-Arm-Systems: Mechanical vibration - Measurement and evaluation of coupling forces to assess the vibration load on the hand-arm system*. DIN Deutsches Institut für Normung e. V., Berlin, Feb, p. 45679.
- Nataletti, P., Marchetti, E., Lunghi, A., Pinto, I., Stacchini, N., Santini, F., 2008. Occupational exposure to mechanical vibration: the Italian vibration database for risk assessment. *International journal of occupational safety and ergonomics : JOSE* 14 (4), 379–386. <https://doi.org/10.1080/10803548.2008.11076775>.
- DIN CEN ISO/TR 7250-2 DIN SPEC 91279:2013, Aug. 2013. *Wesentliche Maße des menschlichen Körpers für die technische Gestaltung – Teil 2: Anthropometrische Datenbanken einzelner nationaler Bevölkerungen: Basic human body measurements for technological design – Part 2: Statistical summaries of body measurements from national populations*. DIN - Deutsches Institut für Normung, Berlin, pp. 7250–7252.
- Rademacher, A., Küffer, G., Spengel, F., 1993. "Vibration white finger"-Syndrom bei acht Schleifern eines großen metallverarbeitenden Betriebes. *Oktober Medizinische Klinik Organ der deutschen Gesellschaft für innere Medizin* 10, 568–570. <https://doi.org/10.5282/ubm/epub.7087>, 1993.
- Rakheja, S., Wu, J.Z., Dong, R.G., Schopper, A.W., 2002. "A comparison of biodynamic models of the human hand-arm system for applications to hand-held power tools. *Journal of Sound and Vibration* 249 (1), 55–82. <https://doi.org/10.1006/jsvi.2001.3831>.
- Scarpa, F., Giacomini, J., Zhang, Y., Pastorino, P., 2005. "Mechanical performance of auxetic polyurethane foam for antivibration glove applications," *cellular polymers*. September (24), 253–268. <https://doi.org/10.1177/026248930502400501>, 2005.
- Schroder, T., Lindenmann, A., Hehmann, S., Uhl, M., Gwosch, T., Matthiesen, S., 2020. "A method of determining the separation plane of a knob-shaped measuring handle for the measurement of hand-arm-impedances," in *VDI - wissensforum GmbH (Hg.)*. In: VDI-tagung Humanschwingungen 2020, 8.
- Steffen, O., Kaulbars, U., 2017. Messen von Ankopplungskräften zur Beurteilung der Vibrationsübertragung auf die Hände: [Measurement of coupling forces to assess vibration transmission to the hands (author transl. " *Technische Sicherheit*, pp. 41–46. <https://doi.org/10.5771/9783845276021-46>, 01/02.
- Verberk, M.M., Salli, H.J.A., Kempers, O., 1985. Vibratory and tactile sense of the fingers after working with sanders. *September International Archives of Occupational and Environmental Health* 56, 217–223. <https://doi.org/10.1007/BF00396599>, 1985.
- Vergara, M., Sancho, J.L., Rodríguez, P., Pérez-González, A., 2008. "Hand-transmitted vibration in power tools: accomplishment of standards and users' perception. *International Journal of Industrial Ergonomics* 38 (9), 652–660. <https://doi.org/10.1016/j.ergon.2007.10.014>.
- Vihlborg, P., Bryngelsson, I.-L., Lindgren, B., Gunnarsson, L.G., Graff, P., 2017. Association between vibration exposure and hand-arm vibration symptoms in a Swedish mechanical industry. *International Journal of Industrial Ergonomics* 62, 77–81. <https://doi.org/10.1016/j.ergon.2017.02.010>.
- Wahl, U., Kaulbars, U., Ernst, F., Hirsch, T., 2019. Vibrationsyndrom der Finger. *Trauma Berufskrankh* 21 (4), 276–285. <https://doi.org/10.1007/s10039-019-00444-1>.
- Wakula, J., Berg, K., Schaub, K., Bruder, R., 2009. *Der Montagespezifische Kraftatlas: [The Assembly-specific Force Atlas (Author Transl. Sankt Augustin. BGLA; Technische Informationsbibliothek u. Universitätsbibliothek, Hannover [Online]. Available: <http://edok01.tib.uni-hannover.de/edoks/e01fn10/61675180X.pdf>*.
- Welcome, D., Rakheja, S., Dong, R., Wu, J.Z., Schopper, A.W., 2004a. An investigation on the relationship between grip, push and contact forces applied to a tool handle. *International Journal of Industrial Ergonomics* 34 (6), 507–518. <https://doi.org/10.1016/j.ergon.2004.06.005>.
- Welcome, D., Rakheja, S., Dong, R., Wu, J.Z., Schopper, A.W., 2004b. An investigation on the relationship between grip, push and contact forces applied to a tool handle. *International Journal of Industrial Ergonomics* 34 (6), 507–518. <https://doi.org/10.1016/j.ergon.2004.06.005>.
- Xu, X., Welcome, D., McDowell, T., Wu, J., Wimer, B., Warren, C., 2011. The vibration transmissibility and driving-point biodynamic response of the hand exposed to vibration normal to the palm. *International Journal of Industrial Ergonomics* 41 (5), 418–427. <https://doi.org/10.1016/j.ergon.2011.05.007>.

Repository KITopen

Dies ist ein Postprint/begutachtetes Manuskript.

Empfohlene Zitierung:

Schröder, T.; Lindenmann, A.; Hehmann, S.; Wettstein, A.; Germann, R.; Gwosch, T.; Matthiesen, S.

[Use of data-driven design for the development of knob-shaped handles in the context of impedance measurements.](#)

2021. Applied ergonomics, 98

[doi:10.5445/IR/1000138842](https://doi.org/10.5445/IR/1000138842)

Zitierung der Originalveröffentlichung:

Schröder, T.; Lindenmann, A.; Hehmann, S.; Wettstein, A.; Germann, R.; Gwosch, T.; Matthiesen, S.

[Use of data-driven design for the development of knob-shaped handles in the context of impedance measurements.](#)

2021. Applied ergonomics, 98, Article no: 103575.

[doi:10.1016/j.apergo.2021.103575](https://doi.org/10.1016/j.apergo.2021.103575)

Lizenzinformationen: [KITopen-Lizenz](#)